



Cucurbitacin E Glucoside-Infused Nanoparticle Membranes for Heavy Metal Removal



Nora O Daoud^a, Wael M Aboulthana^b, Hosny Ibrahim^a, Aida L El-Ansary^a, Heba M Abdallah^c,

^a Department of Chemistry, Faculty of Science, Cairo University, Giza 12613, Egypt

^b Biochemistry Department, Biotechnology Research Institute, National Research Centre, 33 El Bohouth St. (Former El Tahrir St.), P.O. 12622, Dokki, Giza, Egypt

^c Chemical Engineering & Pilot Plant Department, Engineering and Renewable Energy Research Institute, National Research Centre, Giza 12311, Egypt

Abstract

Human life depends on clean water, but even very low levels of heavy metals in water can have negative impacts on both people and the environment, such as increased mortality rates for living things and pollution of the environment. In this study, nanostructure membranes of polyvinyl chloride (PVC) blended with Cucurbitacin E glucoside (CEG-NPs) with different compositions (CM2, CM3, and CM4) were prepared, characterized, and used for the removal of heavy metals ions such as Cu^{+2} , Pb^{+2} , and Ni^{+2} . The synthesized membrane was characterized and verified by H-NMR analysis, SEM, EDX, FTIR, and UV-visible absorption spectra. The results obtained by the synthesized blended membranes showed that CM3 with 0.5 g cucurbitacin E glucoside has a promising performance and has the highest metal removal efficiency, with rejection percentages for Pb^{+2} , Ni^{+2} , and Cu^{+2} reaching 97.6%, 96.4%, and 91.3%, respectively. The rejection flux for this membrane was the highest with an LMH value of 114.12 LMH.

Keywords: Polyvinylchloride (PVC); Cucurbitacin E glucoside; (CEG); Blend Membrane; Heavy Metals ions.

1. Introduction

Our world is experiencing a water shortage; according to the Water Research Institute, Global water demand for agriculture will increase by 60% by 2025, with fresh water making up only 2.53% of total water bodies [1]. Therefore, it is essential that new water treatment techniques be created immediately. Precipitation, oxidation, carbon adsorption, solvent extraction, flotation, evaporation, ion exchange, membrane filtration, phytoremediation, electrochemistry, and biodegradation are some of the technologies that have been employed to treat water [2]. Membrane separation has gained popularity recently because of its benefits, which include low material costs, flexibility, easy scale-up, and ease of fabrication [3]. Nanomembrane technology provides a great opportunity for heavy metal removal in wastewater. Some types of nanomembranes rely on the polymer used for metal removal, such as nano-composite membranes, nanofiber membranes, polyethersulfone (PES) mixed matrix membranes, and polyvinylchloride (PVC) treatment. The drawback of employing these membranes is that all the applied polymers must entirely dissolve in an appropriate organic solvent. Additionally, different types of nanomembranes may encounter some disadvantages, which are briefly discussed so that this technology can be widely used in providing clean water [4]. Nanomembranes can be obtained by different methods, such as anodization, lithography, micromachining, and layer-by-layer deposition. Although the anodization method has the advantage of controlling pore size, its fabrication involves the use of toxic materials. The micromechanical method is very simple, but it requires expensive equipment, and the lithography method is flexible, but the fabrication equipment is very costly. The layer-by-layer approach requires a lot of steps and is time-consuming [5].

Numerous factors, including fabrication techniques and managing the proportions of organic materials, can significantly impact the mechanical properties and porosity of nanomembrane fabrications [5]. There are inverse relations between porosity, permeability, bioactivity, and mechanical properties [7]. Nanomembrane, which has better mechanical prosperities and is biocompatible, needs some modifications. The phase inversion method is the suitable technique for the preparation of polymeric membranes starting from microfiltration membranes with high porosity structures to less porous reverse osmosis membranes. During this process, a polymer is converted from liquid to solid form, making it more convenient for the industry. Different techniques can be employed in the phase inversion method for preparing the membranes, with immersion precipitation being the most commonly used method commercially [8]. In this method, a solid polymer that is already dissolved in a liquid solvent is cast onto a suitable support and then immersed in a coagulation bath containing a non-solvent. The exchange of solvent and non-solvent leads to the formation of the polymer. Recently, researchers have shown interest in synthesizing eco-friendly membranes containing plant extracts and natural products for various applications. For instance, Albukhari et al. (2019) utilized *Duranta leaves's* extract as a reducing agent to synthesize silver nanoparticles (AgNPs).

*Corresponding author e-mail: nora.omar862@gmail.com (Nora O Daoud).

Receive Date: 12 January 2025, Revise Date: 07 March 2025, Accept Date: 16 March 2025

DOI: 10.21608/ejchem.2025.352564.11158

©2025 National Information and Documentation Center (NIDOC)

Cellulose acetate filter paper was modified with titanium dioxide nanoparticles to effectively remove organic dyes from wastewater [9].

Moradi et al. (2020) [10] prepared a membrane by blending boehmite nanoparticles with *curcumin* into a Polyethylene sulfone polymer. They utilized this membrane for the removal of heavy metals from wastewater. Mondal et al. (2019) [11] utilized *clove* extract as both a reducing and surface coating agent. They synthesized an iron-aluminum nanocomposite and investigated its effectiveness in removing fluoride from water. In this study, we utilized cucurbitacin E glucoside extracted from *Citrullus colocynthis*, obtained from the local market. *C. colocynthis* is a perennial herb typically found in desert regions [12]. The fresh fruits of *C. colocynthis* are round and green, turning a different color upon drying. The fruit has a smooth texture and a bitter taste, and it typically contains around 200-300 seeds [13]. Cucurbitacins, reported as the main components of *C. colocynthis* fruits, are highly oxidized tetracyclic triterpenoids. Cucurbitacin E glucoside is categorized as a tetracyclic cucurbitane nucleus skeleton triterpene, unique to cucurbitacins. The structure of triterpenes consists of six isoprene units [14]. As shown in Fig.1, the structure of Cucurbitacin E glucoside explains its hydrophobic properties, and poor water solubility [15]. Therefore, our study aims to evaluate the efficiency of a polyvinyl chloride polymer membrane blended with cucurbitacin E glucoside extracted from *C. colocynthis* and its ability for heavy metal removal.

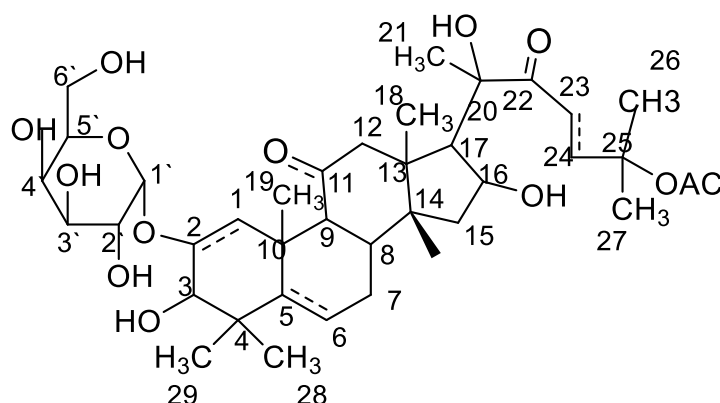


Fig. 1. The structure of E glucose derivative of Oxidaneyl-oxo-(propenyloxy) pentenyl dimethyl(oxidaneyl)-decahydrocyclopentaphenanthredione

2. Experimental (Materials and Methods)

Polyvinyl chloride (PVC), the main polymer, (Roth India Company). Polyethylene glycol 400 (PEG) for pore formation (Sigma-Aldrich). N-methylpyrrolidone (NMP) as a solvent (Fluka). Nickel chloride, copper sulfate, and lead nitrate (Merck). Ethanol, used as a solvent for the extraction of cucurbitacin (Merck).

Extraction of Cucurbitacin

Citrullus colocynthis fruits were obtained from local markets and stored in sealed aluminum foils to be ready for extraction. The extraction method was carried out following the method of Tannin-Spitz et al. (2007) [16] with appropriate modifications. Initially, the *Citrullus Colocynthis* fruits were cleaned with tap water, dried, and grinded to a powder. Five grams of the dry powder were then refluxed in a mixture of chloroform and ethanol (1:9) in an oven at 60°C for 24 hours. The extract was concentrated under reduced pressure, resulting in a yellowish -brown residue.

Membrane Preparation

Different weights of Cucurbitacin E glucoside extracted from *Citrullus colocynthis* were added to 84 g of NMP 1 g of PEG is then added to enhance pore formation and hydrophilic characteristic. the mixture was stirred gently for 60 min, and then vigorously stirring using mechanical stirrer. During stirring, 14 g of polyvinyl chloride (PVC) was gradually added until completely dissolved. The stirring was continued overnight. A list of the polymeric solutions composition is given in Table 1, Polyvinyl Chloride can be abbreviated as PVC, Polyethylene Glycol, as PEG, N-methyl-2-pyrrolidone as NMP, Cucurbitacin E glucoside as CM, Blank membrane as BM1, and various ratios of Cucurbitacin E glucoside were denoted as CM2, CM3, and CM4.

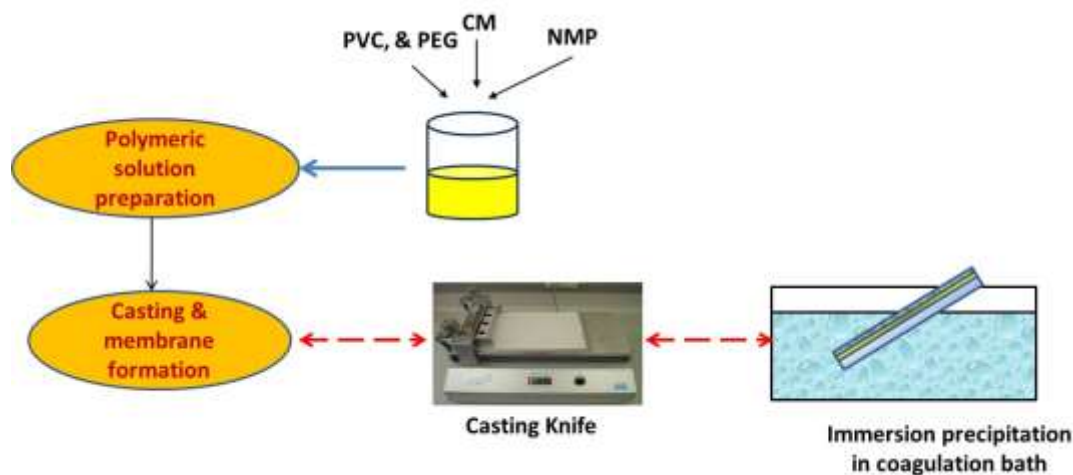


Fig. 2. Graphical mechanism of membrane preparation

Figure 2 showed the steps involved in preparing the membrane, where after polymeric solution preparation it was cast on a nonwoven polypropylene fabric support to enhance the membrane mechanical structure.

Table. 1: The composition of polymeric solutions percentages

Polymeric Membrane	Composition (weight percent)			
	PVC %	PEG %	NMP %	CM %
BM1	14	1	85	0
CM2	14	1	84.7	0.3
CM3	14	1	84.5	0.5
CM4	14	1	84	1

Characterization of Cucurbitacin

The characterization of Cucurbitacin E glucoside extracted from *Citrullus colocynthis*, was conducted using UV-visible double-beam spectrometry (Carry 60, 200-800 nm) and NMR analysis, with an NMR spectrometer (Varian 300MHz, acetone-H1 at 30°C).

Fourier Transform Infrared Spectroscopy (FTIR)

The polymeric membrane was analyzed using a JASCO-FTIR 4100 spectrophotometer to gather information about chemical bonding and molecular structure. The analysis was conducted in the range of 4000–400 cm^{-1} .

Mechanical Properties

Various techniques were employed to determine the properties of the synthesized membrane, including assessing mechanical properties and membrane thickness. These techniques are suitable for studying the viscous behavior of the synthesized polymeric membranes under different environmental conditions. The mechanical properties testing system (H5KS) and a universal testing machine were utilized to analyze the properties of the membranes. The membrane samples were 10 cm in length and 2.5 cm in width. Tensile strength and elongation were measured at a rate of 5 cm/min for all samples. The average value of three samples for each membrane was recorded, and the thickness of the samples was measured using a plastic film thickness gauge. The final thickness of the prepared membrane was consistent at 1×2.5 cm for all ratios of the prepared membrane.

Porosity Measurements

Membrane porosity can be defined by the equation [1] as the total volume of the membrane pores divided by the volume of the holes. Abdallah et al. (2021) reported that the porosity of membranes can be calculated as a function of membrane weight. The different weights of the membrane were recorded when dry and then wet. Firstly, the prepared membranes were immersed in ultrapure water for 24 hours, and the weight, M1, was recorded. They were then allowed to dry in an oven for 24 hours at 100 °C, and the weight M2 was recorded.

$$\text{Porosity} = [(M1 - M2) / (A d \rho)] 100 \text{ ----- [1]}$$

Where A is the membrane area, d represents the membrane's thickness, and ρ is the water's density. M1 and M2 are the weights of the wet and dry membrane.

Membrane Performance Testing

The membrane performance testing was conducted in dead-end filtration mode using a system with an effective membrane area of 19.2 cm². The process was conducted at 5 bar pressure for 1 hour. The system included a feeding flask, a pump, valves, pressure gauge, and a membrane module as shown in Fig. 3.

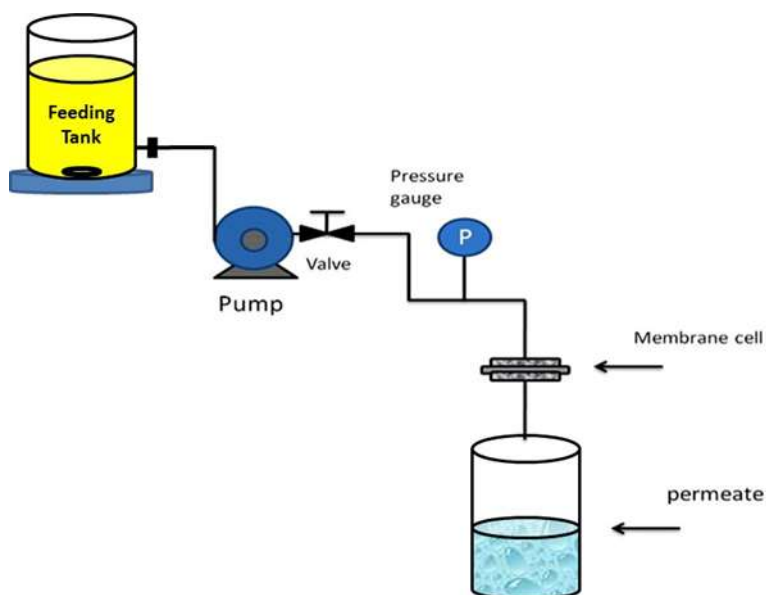


Fig.3. Membrane testing system

Heavy Metals Removal

To remove various metals such as Cu²⁺, Pb²⁺, and Ni²⁺ using the filtration technique, the process involved inserting membranes into a closed filtration system inside a cell under a pressure of 8 bar. Initially, ultrapure water was circulated through the system without any membranes. The water flux was recorded every 10 minutes during 1 hour of filtration using the following equation [2]:

$$F = W / (A)(t) \text{ (kg/m}^2\text{h)} \text{ ----- [2]}$$

Where W is the weight of collected water at the permeate side (kg), A is the membrane area (m²), and t is the filtration time (h). To conduct the experiment, solutions containing Cu²⁺, Pb²⁺, and Ni²⁺ (10 mg/L of each) adjusted to pH 5, were fed to the system and the concentrations of each element was measured in the collected solutions using inductively coupled plasma atomic emission spectroscopy (ICP-AES). The amount of rejected heavy metals was calculated using the equation [3].

$$R \% = (1 - C_p / C_f) 100 \text{ ----- [3]}$$

Where C_p and C_f are the concentrations of each ion present in permeate and feed solutions, respectively.

Membrane Fouling Test

A membrane of composition (CM3) was used to evaluate the membrane fouling. The test was carried out using the same equipment as the membrane performance test. The dead-end mode system was employed to expose the membrane surface to perpendicular flow, which could result in clogging and pore size formation on the surface. The feed solution for this test contained 50 mg/L of Cu²⁺, Pb²⁺, and Ni²⁺. The permeate flux was monitored to track the flux variation over time. Pure water was passed through the membranes for 30 min then heavy metal solution passing through the membrane for 1 hour, followed by ultra-pure water 30 min again, and the flux was recorded. This sequence was repeated continuously.

Adsorption Capacity

The adsorption capacity of the prepared membranes to remove Cu²⁺, Pb²⁺, and Ni²⁺ from aqueous solutions was tested. 50 mL of Cu²⁺, Pb²⁺, and Ni²⁺ with a concentration of 10 mg/L at 25°C were placed on a shaker at 400 rpm for 24 hours. The adsorption amount of metal ions on the membrane (mg/g) was calculated using the following equation [4]:

$$Q = (C_0 - C_e) V / M \text{ ----- [4]}$$

Where Q is the adsorption amount of metal ions on the membrane (mg/g), C₀ and C_e are the starting and equilibrium concentrations of metal ions (mg/l), respectively. V is the solution volume, and M is the membrane weight.

3. Results and Discussion

¹H-NMR Spectral Analysis

Analytical data for Cucurbitacin E glucoside was compared with the literature by Hussein, et. al. (2017). The proton, ¹H-NMR of the extract in our study dissolved in dehydrated acetone as the solvent.

The ¹H-NMR spectral properties of isolated Cucurbitacin E glucoside results are similar to those reported by Hussein et al., (2017), with the AC proton at 4.014, H 8 at 2.509 [18]. The shifts in results for protons 7, H 9, H 15, H 17, H 18, and H 19, attributed to the use of different solvents and apparatus [19].

UV-Visible Spectroscopy

The UV-visible absorption spectra of isolated Cucurbitacin E glucoside show a broad band at λ_{max} of 255 nm in Fig. (4a), indicating the presence of the compound, this is consistent with the results reported by Metcalf et al., (1982). In Fig. (4b), the UV-visible absorption spectra of PVC polymer as a blank and PVC polymer blended with Cucurbitacin E glucoside show the absorption band at λ_{max} = 360 nm, and 370 nm for PVC, and CEG/PVC, respectively, with a red shift to longer wavelengths. This indicates bond formation between (the PVC) polymer and Cucurbitacin E glucoside.

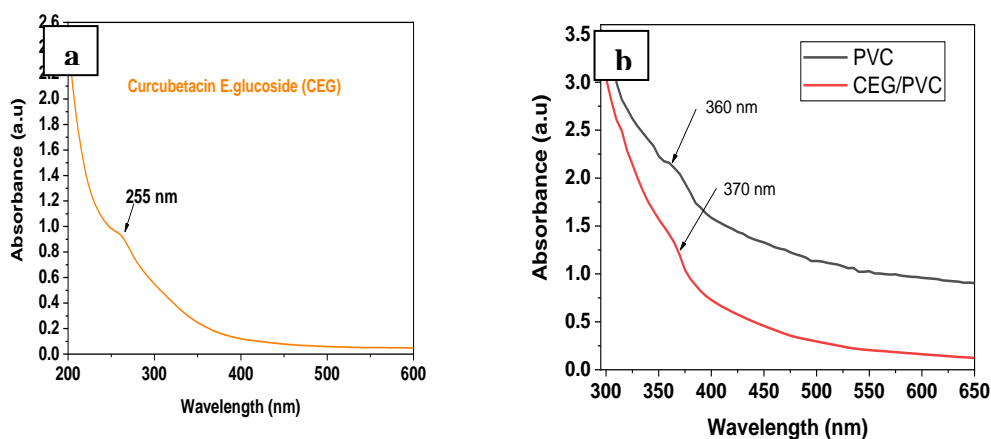


Fig.4. UV- visible absorption spectra of (a) CEG-NPs., and (b) CEG/PVC-NPs

Fourier Transform Infrared Spectroscopy (FTIR)

Comparing the FTIR spectra of PVC polymer (as blank) and CEG/PVC (Fig. 5) reveals that the signals at 1238, 1159, 1102, 951, and 862 cm^{-1} are attributed to PVC polymer. The peak at 607 cm^{-1} corresponds to stretching in the C-Cl bond, while the peak at 1719 cm^{-1} is associated with C=O stretching. The peaks observed in the range of 2920–2850 cm^{-1} are a result of C-H stretching of aliphatic groups. Changes in peak intensity and broadening suggest the formation of intra- and intermolecular H-bonding. It is evident that most peaks in the blended membrane samples exhibit a shift and lower intensity. The strong backbone of PVC is attributed to its long aliphatic chain. The chemical properties of PVC undergo changes during synthesis, leading to a high yield. The presence of chlorine site along the polymer chain, as a leaving group facilitates chemical modification.

The addition of Cucurbitacin E glucoside to PVC enhances the polymer's strength through bond formation between Cucurbitacin E glucoside and PVC. This bond changes PVC properties such as surface charge, hydrophilicity, and mechanical properties. Accordingly, the red shift in UV absorption wavelength shown in Fig. 4b and the red shift in the wavelength of the IR spectrum of the C-Cl bond shown in Fig. 5, indicate a bond formation between PVC and Cucurbitacin E glucoside as shown in Fig. 6. These findings are corroborated by Ameer et. al. (2013).

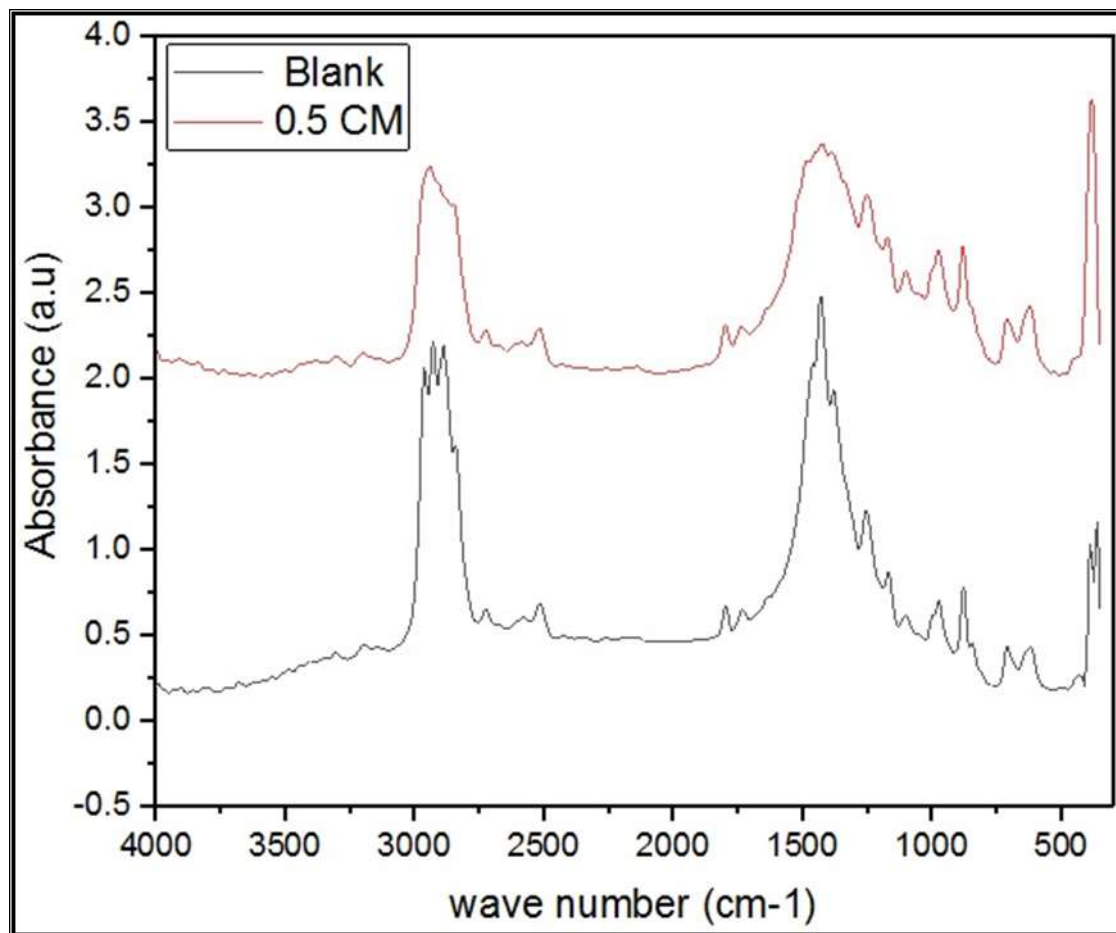


Fig. 5. FTIR of the BM membrane and CM3

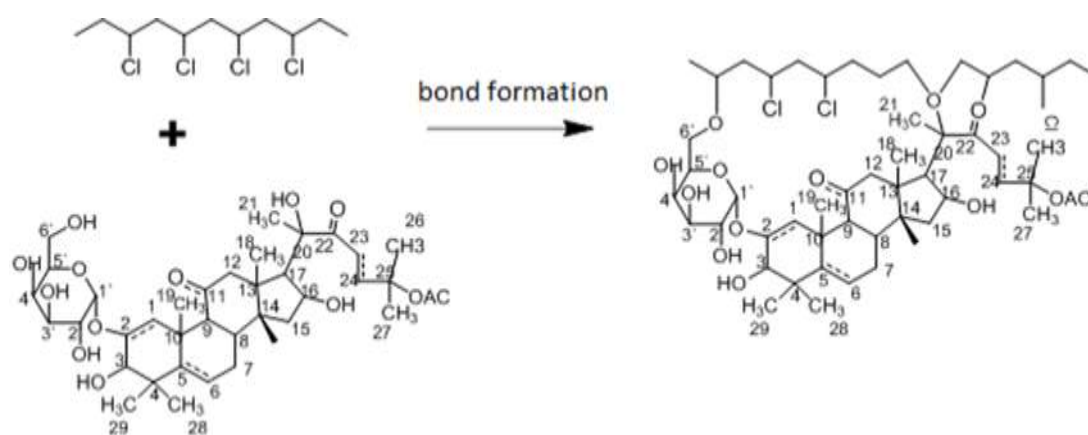


Fig.6. Schematic diagram of bond formation between PVC and CEG

Mechanical Properties

Fig. 7. Shows the results and investigation of the mechanical properties of the prepared membranes, namely BM1, CM4, CM2, and CM3, depending on the amount and ratios of extracted Cucurbitacin E glucoside. It is clear that the quality of the prepared membrane CM3 provides the highest tensile strength of $9.8.3 \pm 0.05$ MPa, with an elongation percentage of $78.5 \pm 0.1\%$, while the lowest mechanical properties, tensile strength, and elongation are showed up with BM1 with values of 7.8 ± 0.05 MPa and $59.3 \pm 0.2\%$, respectively. The tensile strength of the membranes increases in the following order: $BM1 < CM4 < CM2 < CM3$. Also, it shows that the highest value is for CM3, which was prepared from PVC 14 wt%, PEG 1 wt%, and 0.5 wt% of extracted cucurbitacin E glucoside. The elongation of the membranes increases in the following order: $BM1 < CM4 < CM2 < CM3$. Cucurbitacin E glucoside reacts with the PVC polymer, creating a crosslinking matrix in the membranes. The linking between polymer chains and Cucurbitacin E glucoside particles leads to an increase in the strength of the polymer chains, which acquire more energy to break down the bonds between them [22].

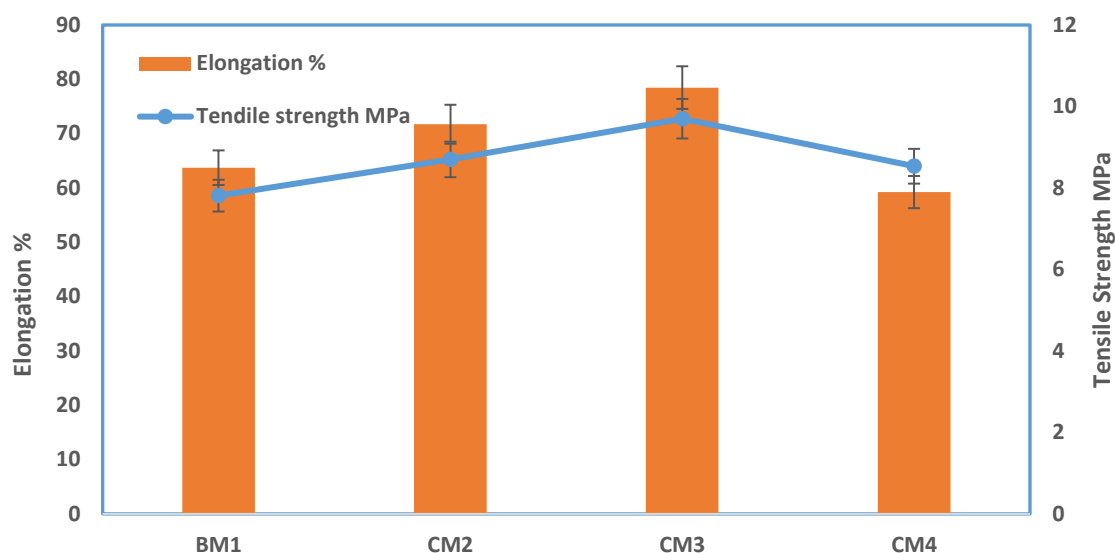


Fig. 7. The mechanical properties and elongation for different membranes.

Porosity

Table 2 shows the porosity values of the studied membranes. CM4 has the lowest porosity at $11.53 \pm 0.5\%$ as a result of containing the highest extract percentage, while BM1 has the highest porosity at $31.12 \pm 0.52\%$ because it contains no extract. Increasing the extract percentage leads to a shrinkage in the pores, which has an effect on decreasing membrane porosity. This results in an overall size reduction and decreases porosity of the pores, enhancing the mechanical properties of the membranes [23].

Table 2: The overall porosity and thickness of prepared membranes

Membranes	Thickness (mm)	Porosity %
BM1	0.17	31.12
CM2	0.18	16.82
CM3	0.17	13.18
CM4	0.15	11.53

Scanning Electron Microscope

Fig. (8 a, b and c) illustrates the top surface morphology of the membranes. Image a shows the BM1 membrane (PVC-membrane without extract), the image shows that this blank membrane has the wider pores. SEM image (b) for CM3 membrane containing 0.5% of curcubitacin, revealed that the membrane has particles uniformly distributed on its surface. The pore size in CM3 is much smaller than in BM1 due to bond formation between the PVC chain and curcubitacin particles. The distribution of pores in the membranes affects rejection; the more uniformly distributed, the higher the rejection [22]. Using Cucurbitacin E glucoside fine particles during polymeric solution preparation increase the viscosity of the liquid which leads to quick liquid-liquid phase separation forming porous membrane's structure. So, the phase inversion process ideally provided pores on the membrane surface through solvent evaporation to coagulation bath [24]. Fig. (8c) shows the surface's morphology of the CM3 membrane after filtration of solution containing Cu^{+2} , Pb^{+2} and Ni^{+2} ions. The pore size didn't change, and the membrane is brighter than before due to the presence of heavy metal ions.

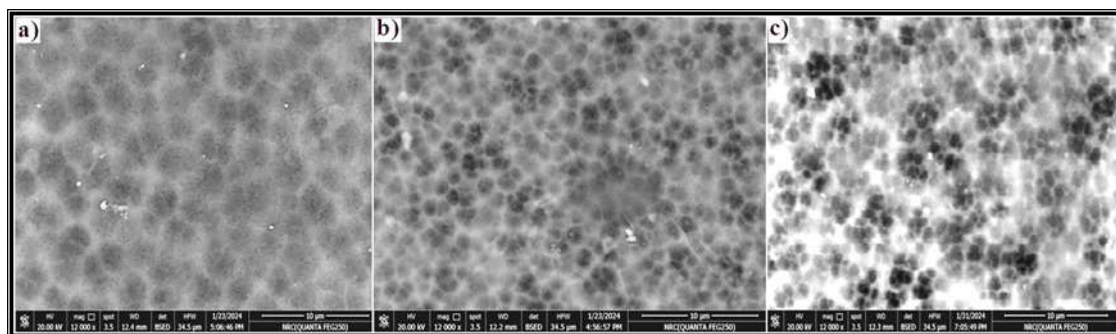


Fig. (8a, b, c). SEM, showing (a) blank membrane, (b) CM3 with 0.5 % Cucurbitacin, and (c) CM3 membrane after filtration of Cu^{+2} , Pb^{+2} and Ni^{+2} solution.

EDXS

Energy dispersive X-ray spectroscopy (EDX) is used to determine the relative amounts of each element in membranes as well as their compositions. It verifies that elements of carbon, oxygen, and chloride are present. Fig. (9a, b, and c) demonstrate a rise in the chlorine percentage, which suggests a greater negative charge in the membrane and makes it more favorable for metal adsorption. There are two ways for the membrane to remove heavy metals: chemical and physical adsorption, in our case, it's mainly van der Waals physical adsorption [25]. EDXS results for the CM3 polymeric membrane confirm the presence of elements such as copper, nickel, and lead after filtration of the solution containing these ions.

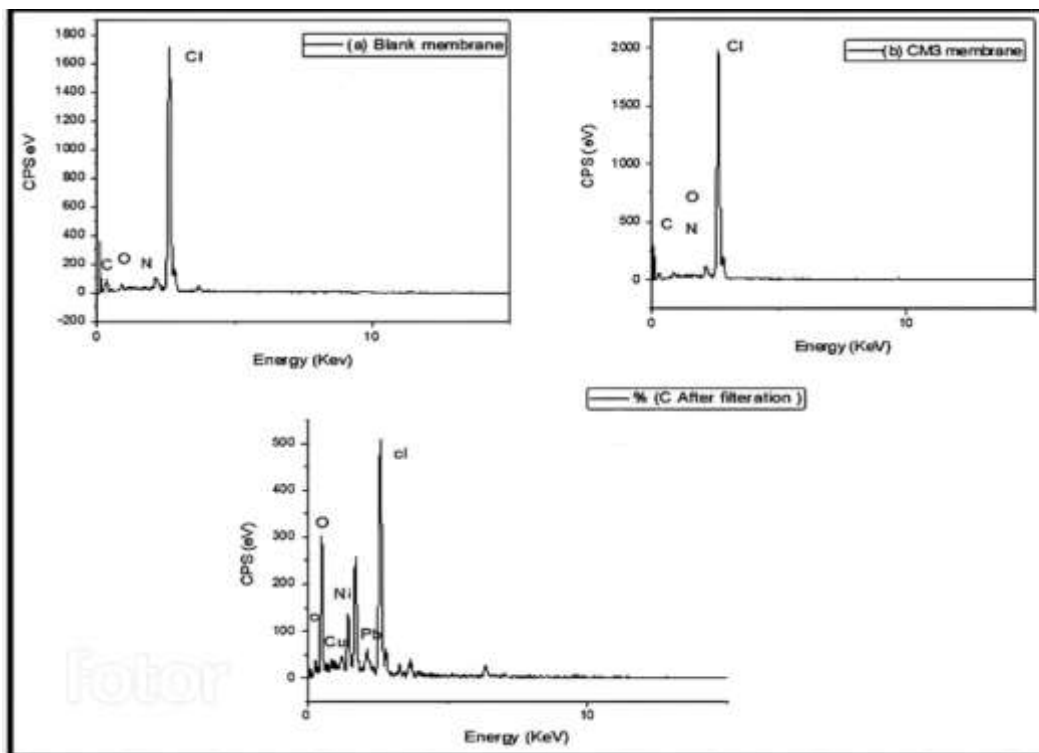


Fig. (9a, b, and c). EDX, for the blank PVC membrane (a) CM3 nanocomposite membrane (b) and CM3 with heavy metals (c).

Heavy Metals Removal

Fig. (10 a, b, c, and d) shows the rejection percentages of Cu^{+2} , Pb^{+2} , and Ni^{+2} ions, which were calculated from concentrations measured by inductively coupled plasma atomic emission spectroscopy (ICP-AES), this achieved using the filtration technique under a pressure of 8 bar for 1 hour. The CM3 membrane exhibited higher rejection percentages, with 97.6% for Pb^{+2} , 96.4% for Ni^{+2} , and 91.3% for Cu^{+2} . The rejection flux for CM3 was 114.12 LMH, the highest among the membranes tested, followed by CM2 with 58.2 LMH, CM4 with 54.11 LMH, and BM with 45.29 LMH flux. The BM membrane, which did not contain any CEG, had the lowest rejection percentages at 32.2% for Pb^{+2} , 35% for Ni^{+2} , and 18.2% for Cu^{+2} . The blending of Cucurbitacin E glucoside to PVC polymer increased the negative charge of the prepared membrane, enhancing the electrostatic attraction between positive metal ions and the membrane.

Active oxygen can chelate metal ions, increasing the rejection percentage. The effective pore size may not always be the actual pore size as membrane efficiency can increase after the rejection of small particles. Large particles adsorbed on the membrane surface can affect the effective pore size, which in turn affects rejection [26].

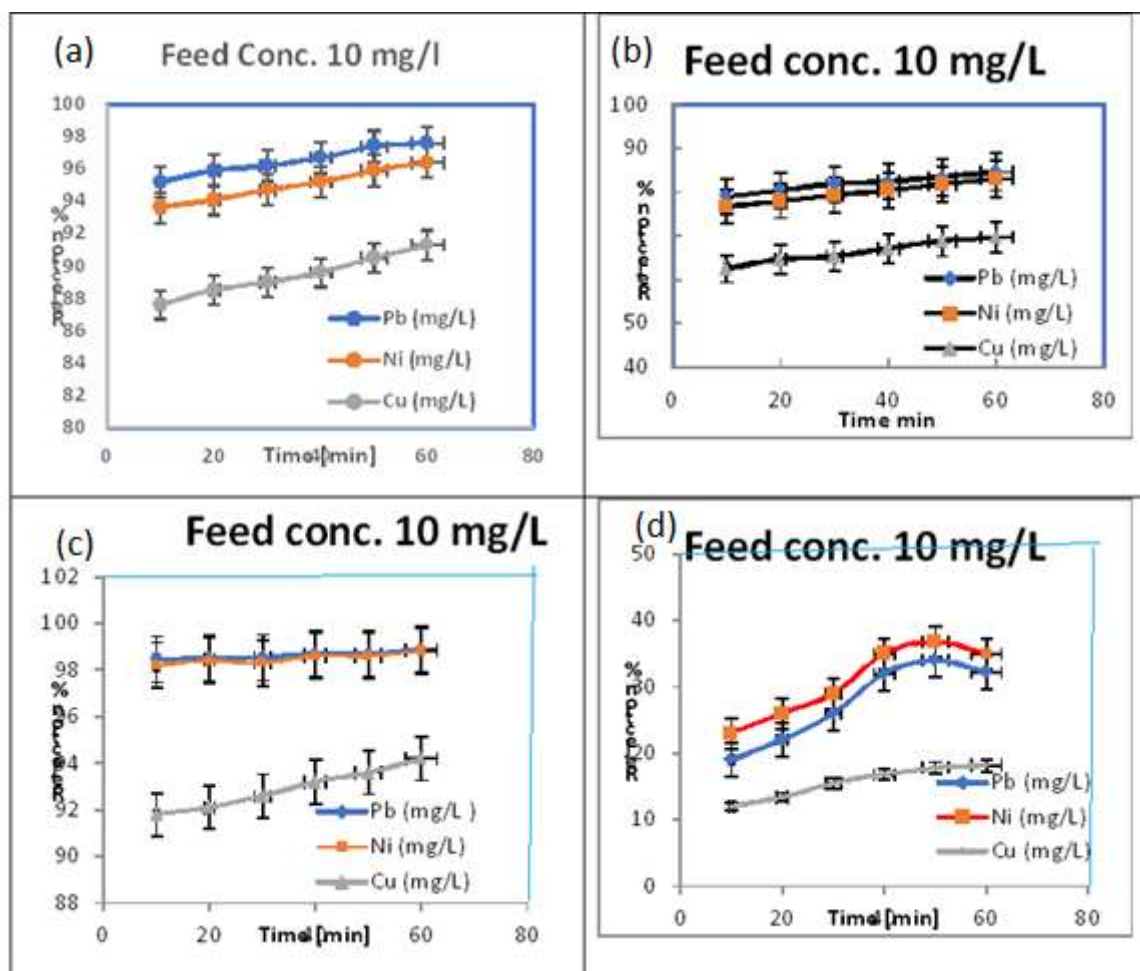


Fig. (10 a, b, c and d) The rejection percentages for Pb^{+2} , Ni^{+2} , and Cu^{+2} ions of (a) CM3 membrane, (b) CM2 membrane, (c) CM4 membrane, and (d) BM membrane.

Adsorption Capacity

The adsorption capacity of the prepared membranes towards Cu^{+2} , Pb^{+2} , and Ni^{+2} was evaluated. A 50 mL solution containing 10 mg/L of Cu^{+2} , Pb^{+2} , and Ni^{+2} was prepared. A known weight of CM3 and BM membranes were added to the solutions separately. After 24 hours of shaking at 400 RPM, the concentrations of Cu^{+2} , Pb^{+2} , and Ni^{+2} were measured, and the adsorption capacity of the membranes for these metal ions was calculated. It was observed that after 24 hours, the active sites of the membrane were saturated. The blank membrane exhibited poor adsorption capacity for heavy metal ions Cu^{+2} , Pb^{+2} , and Ni^{+2} due to the more uniformly distributed main functional groups on its surface and the smaller pore size. As shown in Fig. [11], CM3 had a higher adsorption capacity than the BM membrane due to the contribution of Cucurbitacin E glucoside with PVC. The adsorption capacity of the CM3 membrane for the studied heavy metal ions was in the order of $\text{Pb}^{+2} > \text{Ni}^{+2} > \text{Cu}^{+2}$. The adsorption capacity of Cu^{+2} , Pb^{+2} , and Ni^{+2} adsorbed in the CM3 were 20.5, 19.05, and 18 mg/g, respectively. The adsorption capacity of Cu^{+2} , Pb^{+2} , and Ni^{+2} adsorbed in the BM were 4.3, 3.9, and 2.5 mg/g, respectively.

The adsorption capacity has the order of $\text{Pb}^{+2} > \text{Ni}^{+2} > \text{Cu}^{+2}$. This is due to the electronegativity order of $\text{Pb}^{+2} > \text{Ni}^{+2} > \text{Cu}^{+2}$. The hydrated radii order of $\text{Pb}^{+2} < \text{Ni}^{+2} < \text{Cu}^{+2}$. Pb^{+2} has a lower hydrated radius and higher electronegativity, resulting in a higher adsorption percentage [27].

The attachment of metal ions to the studied membranes can be explained according to the following bases. Active sites as reported by Kapoor et. al. (2020) [28-30] include OH at positions 3', 6', and 20, and O atom at position 22, which can chelate metals or bond to PVC polymer as shown in Fig. [12]. Reactive oxygen species can initiate the peroxidation of membranes, leading to the accumulation of peroxide radicals. These reactive oxygen species are responsible for the removal of heavy metals. In the present study, we demonstrated that reactive sites such as, hydroxyl radicals, superoxide anions, and singlet oxygen radicals present in membranes blended with CEG are able to scavenge metal ions [16].

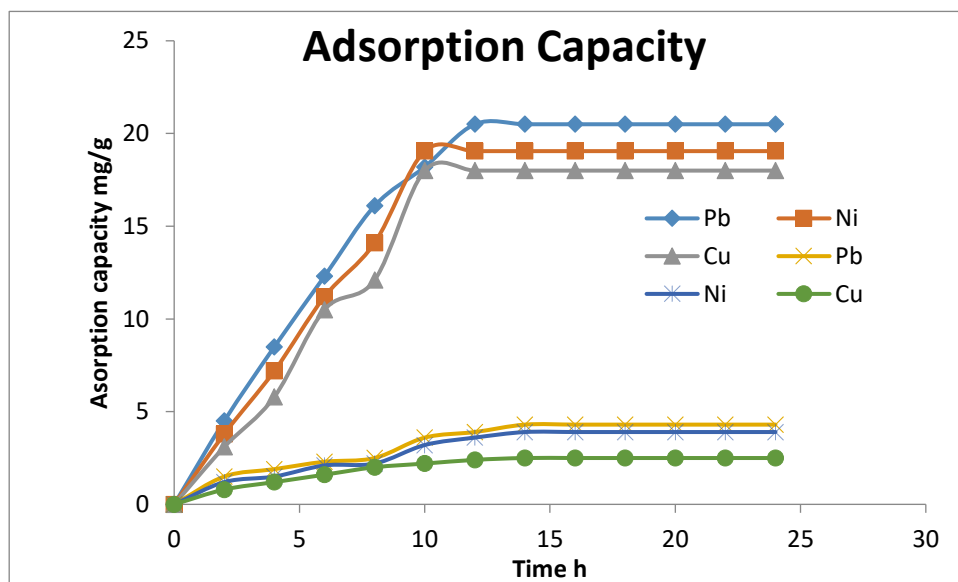


Fig.11. The adsorption capacity of Cu^{+2} , Pb^{+2} , and Ni^{+2} on CM3 and BM

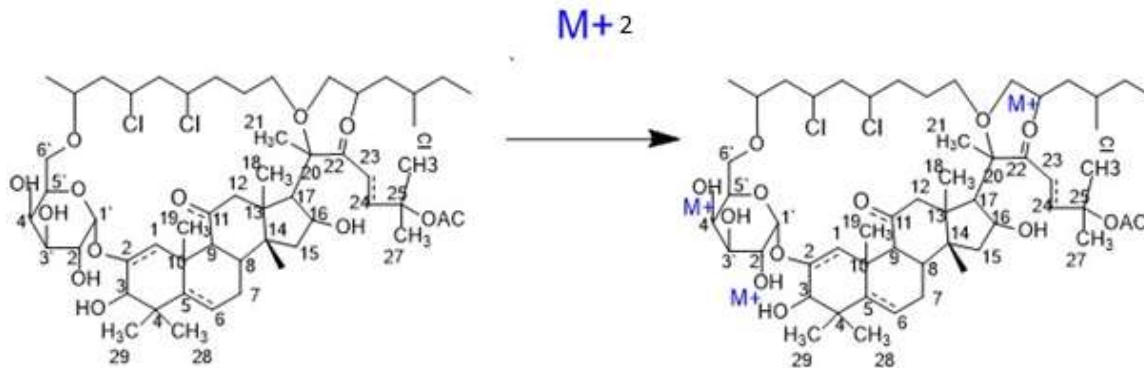


Fig. 12. Cation reaction of metal ions with active site of CEG/PVC

Membrane Fouling Test

Fouling greatly depends on the choice of the membrane material, particularly its surface chemistry and porous structure. Numerous studies focus on improving the hydrophilicity of membranes to prevent hydrophobic contaminants from sticking to the surface [31-34]. The fouling experiment of the CEG/PVC membrane was evaluated through a three-cycle filtration test [17] of a heavy metals solution, and the permeate flux and the results are illustrated in Fig.14. Fouling experiment aimed to test the membrane stability. The first 30 minutes of the test involved washing with deionized water, followed by replacing the feed with 50 ppm of Cu^{+2} , Pb^{+2} , and Ni^{+2} solution, and then washing the membrane with distilled water for another 30 minutes. This process was repeated using distilled water and metal ions solution alternatively, for 6 hours. This experiment was conducted only for the CM3. The membrane's performance was good, with a stable heavy metal rejection flux of approximately 80.0 LMH. The flux increased after washing with deionized water and then returned to its stable state. Furthermore, after the filtration process and cleaning, the membrane still exhibited a good water flux of ≈ 115.0 LMH. In general, the prepared CM3 blend membrane displayed high flux recovery during the filtration process, indicating its good durability property and reusability for the removal of heavy metals.

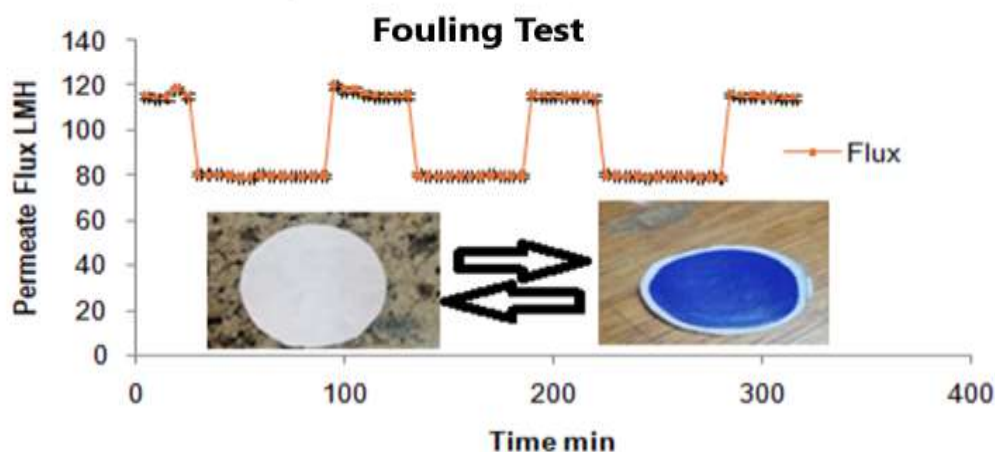


Fig. 13. Fouling experiment for CM3 membrane.

Table 3 shows that different composites were used to prepare various membranes. Some of them utilized nanometals, while others used extractions of natural products, or a combination of both. This affected the flux and rejection percentage, leading to recommendations for the optimal membrane for rejection.

Table 3: Comparative study of the prepared membrane with previously developed membranes

Comparative Property	Previous Membranes			Present Membrane
	Pectin/magnetite/pine sawdust (PE/Fe ₃ O ₄ /P) [30]	Nickel-bentonite NBNPs/Polyethersulfone (PES) with Scrophularia striata extract.[31]	The PES/B-Cur boehmite nanoparticles with curcumin[10]	Polyvinyl Chloride (PVC) blended with Cucurbitacin E glucoside (CEG-NPs)
Used as	Rejection of Cd ²⁺ , Cr ⁶⁺ , Cu ²⁺ , Mn ²⁺ , Ni ²⁺ , and Zn ²⁺	Removal of Zn ²⁺ , Cu ²⁺ and Pb ²⁺ .	Removal of Fe ²⁺ , Cu ²⁺ , pb ²⁺ , Mn ²⁺ , Ni ²⁺ , and Zn ²⁺ .	Removal of Cu ²⁺ , Pb ²⁺ and Ni ²⁺ .
Optimum Composition Ratio	The membrane with best result was PE/Fe ₃ O ₄ /P5%	The composition of 0.5 wt% of NBNPs, shows best rejections	Membrane with 0.5 wt.% B-Cur nanoparticles was the best performance	Membranf with 0.5 g cucurbitacin E glucoside shows promosing performance
Capacity percentage/ Rejection Percentage	The Cu ²⁺ has highest sorption capacity (~43 mg g ⁻¹).	Rejection percentage were (Zn ²⁺ : 98.62%, Cu ²⁺ : 97.88% and Pb ²⁺ : 97.03%).	. The Fe ²⁺ , Cu ²⁺ , pb ²⁺ , Mn ²⁺ , Zn ²⁺ , and Ni ²⁺ rejection were 99.88, 98.72, 99.61, 99.31, 99.11, and 99.51% respectively	Rejection percentages for Pb ²⁺ , Ni ²⁺ , and Cu ²⁺ reaching 97.6%, 96.4%, and 91.3%, respectively
Flux	No detectable	Water flux was 58.8 kg/m ² h for 0.5 wt% of NBNPs.	water flux was 120-140 kg/m ² h	Rejection flux for membrane with the best performance was 114.12 LMH.

4. Conclusion

Cucurbitacin E glucoside has a significant effect on the morphology, batch adsorption, antifouling behavior, and heavy metal ion rejection. Cucurbitacin E glucoside nanoparticles were synthesized and characterized using ^1H -NMR and FTIR, analysis. Additionally, SEM, EDX, pore size distribution, mechanical properties, and porosity measurements confirmed the presence of Cucurbitacin E glucoside nanoparticles in the membrane matrix, resulting in changes in pore size and porosity, as indicated by FESEM, pore size distribution, and porosity measurements. The synthesized blended membranes results indicate that CM3, containing 0.5 g of cucurbitacin E glucoside, exhibited promising performance. It demonstrated the highest metal removal efficiency, with rejection rates of 97.6% for Pb^{+2} , 96.4% for Ni^{+2} , and 91.3% for Cu^{+2} . Additionally, this membrane had the highest rejection flux, with a value of 114.12 LMH.

Conflict of interest

The authors have no conflict of interest to declare.

Formatting of funding sources

This research did not receive any specific grant from funding agencies in the public, commercial, or not-for-profit sectors.

Acknowledgment

This work was supported by National Research Centre (NRC).

References

- 1 . Boretti, A., & Rosa, L. (2019). Reassessing the projections of the world water development report. *NPJ Clean Water*, 2(1), 15.
- 2 .Crini, G., & Lichtfouse, E. (2019). Advantages and disadvantages of techniques used for wastewater treatment. *Environmental chemistry letters*, 17, 145-155.
- 3 .Zhuang, G. L., Tseng, H. H., & Wey, M. Y. (2016). Feasibility of using waste polystyrene as a membrane material for gas separation. *Chemical Engineering Research and Design*, 111, 204-217.
- 4 .Rozelle, L., Cadotte, J., Corneliussen, R., Erickson, E., Cobian, K., & Kopp Jr, C. (2000). Phase inversion membranes. *Encyclopedia of Separation Science*; Mulder, M., Ed.; Academic Press: Cambridge, MA, USA, 3331-3346.
- 5 . Ciganè, U., Palevičius, A., & Janušas, G. (2021). Review of nanomembranes: Materials, fabrications and applications in tissue engineering (bone and skin) and drug delivery systems. *Journal of Materials Science*, 56(24), 13479-13498.
- 6 . Adiga S, Jin C, Curtiss L, Monteiro-Riviere N, Narayan RJ (2009) Nanoporous membranes for medical and biological applications. *WIREs Nanomed Nanobiotechnol* 1:568–581.
- 7 .-Christy PN, Basha SK, Kumari VS, Bashir AKH, Maaza M, Kaviyarasu K, Arasu MV, Al-Dhabi NA, Ignacimuthu S (2020) Biopolymeric nanocomposite scaffolds for bone tissue engineering applications: a review. *J Drug Deliv Sci Technol*. <https://doi.org/10.1016/j.jddst.2019.101452>
- 8 .Kausar, A. (2017). Phase inversion technique-based polyamide films and their applications: a comprehensive review. *Polymer-plastics technology and engineering*, 56(13), 1421-1437.
- 9 .Albukhari, S. M., Ismail, M., Akhtar, K., & Danish, E. Y. (2019). Catalytic reduction of nitrophenols and dyes using silver nanoparticles@ cellulose polymer paper for the resolution of waste water treatment challenges. *Colloids and Surfaces A: Physicochemical and Engineering Aspects*, 577, 548-561.
- 10 .Moradi, G., Zinadini, S., Rajabi, L., & Derakhshan, A. A. (2020). Removal of heavy metal ions using a new high performance nanofiltration membrane modified with curcumin boehmite nanoparticles. *Chemical Engineering Journal*, 390, 124546.
- 11 .Mondal, P., & Purkait, M. K. (2019). Preparation and characterization of novel green synthesized iron–aluminum nanocomposite and studying its efficiency in fluoride removal. *Chemosphere*, 235, 391-402.
- 12 . Mariod, A. A., & Jarret, R. L. (2022). Antioxidant, antimicrobial, and antidiabetic activities of Citrullus colocynthis seed oil. In *Multiple biological activities of unconventional seed oils* (pp. 139-146). Academic Press.
- 13 . Bhasin, A., Singh, S. and Garg, R., 2020. Nutritional and medical importance of Citrullus colocynthis-A review. *Plant Archives*, 20(2), pp.3400-3406.
- 14 . Alghasham, A. A. (2013). Cucurbitacins—a promising target for cancer therapy. *International journal of health sciences*, 7(1), 77..
- 15 . Gry, J., Soborg, I., & Anderson, H. C. (2006). Identity, physical and chemical properties, analytical methods. Cucurbitacins in plant food. Tema Nord Nordic Council of Ministers. Print: Ekspressen Tryk & Kopicenter. Copenhagen, 556, 17-22.
- 16 . Tannin-Spitz, T., Bergman, M., & Grossman, S. (2007). Cucurbitacin glucosides: Antioxidant and free-radical scavenging activities. *Biochemical and Biophysical Research Communications*, 364(1), 181-186.
- 17 .Abdallah, H., Shalaby, M., Fang, L. F., Zhu, B. K., & Shaban, A. (2021). Mixed Matrix Membranes from Polyvinylchloride and Manganese Organic Complex Compound for Fouling and Viral Resistance. *Journal of Membrane Science and Research*, 7(3), 196-208.
- 18 .Hussein, M. A., El-Gizawy, H. A. E., Gobba, N. A. E. K., & Mosaad, Y. O. (2017). Synthesis of cinnamyl and caffeoyl derivatives of Cucurbitacin-Eglycoside Isolated from Citrullus colocynthis fruits and their structures antioxidant and anti-inflammatory activities relationship. *Current pharmaceutical biotechnology*, 18(8), 677-693.

- 19 .Seger, C., Sturm, S., Mair, M. E., Ellmerer, E. P., & Stuppner, H. (2005). ^1H and ^{13}C NMR signal assignment of cucurbitacin derivatives from *Citrullus colocynthis* (L.) Schrader and *Ecballium elaterium* L.(Cucurbitaceae). *Magnetic Resonance in Chemistry*, 43(6), 489-491.
- 20 .Metcalf, R. L., Rhodes, A. M., Metcalf, R. A., Ferguson, J., Metcalf, E. R., & Lu, P. Y. (1982). Cucurbitacin contents and diabroticite (Coleoptera: Chrysomelidae) feeding upon Cucurbita spp. *Environmental Entomology*, 11(4), 931-937.
- 21 .Ameer, A. A., Abdallah, M. S., Ahmed, A. A., & Yousif, E. A. (2013). Synthesis and characterization of polyvinyl chloride chemically modified by amines. *Open Journal of Polymer Chemistry*, 3(01), 11-15.
- 22 . Shalaby, M., Mansor, E. S., Abdallah, H., Shaban, A. M., Zhu, B. K., & Fang, L. F. (2021). Antiviral amphiphilic membranes based on the organometallic compound for protein removal from wastewater with fouling-resistant. *Journal of Polymer Research*, 28, 1-15
23. Nayak, V., Jyothi, M. S., Balakrishna, R. G., Padaki, M., & Deon, S. (2017). Novel modified poly vinyl chloride blend membranes for removal of heavy metals from mixed ion feed sample. *Journal of hazardous materials*, 331, 289-299.
- 24 . Reuvers, A. J., & Smolders, C. A. (1987). Formation of membranes by means of immersion precipitation: Part II. the mechanism of formation of membranes prepared from the system cellulose acetate-acetone-water. *Journal of membrane science*, 34(1), 67-86.
- 25 .Khulbe, K. C., & Matsuura, T. (2018). Removal of heavy metals and pollutants by membrane adsorption techniques. *Applied water science*, 8, 1-30.
- 26 .Lacey, R. E., & Loeb, S. (2000). Filtration Mechanism. *Desalination*, 28(31), 40.
- 27 .Alsohaimi, I. H., Wabaidur, S. M., Kumar, M., Khan, M. A., Alothman, Z. A., & Abdalla, M. A. (2015). Synthesis, characterization of PMDA/TMSPEDA hybrid nano-composite and its applications as an adsorbent for the removal of bivalent heavy metals ions. *Chemical Engineering Journal*, 270, 9-21.
28. Kapoor, N., Ghorai, S. M., Kushwaha, P. K., Shukla, R., Aggarwal, C., & Bandichhor, R. (2020). Plausible mechanisms explaining the role of cucurbitacins as potential therapeutic drugs against coronavirus 2019. *Informatics in medicine unlocked*, 21, 100484.
29. Sobeh, E. I., El-Ghannam, G., Korany, R. M., Saleh, H. M., & Elfeky, S. A. (2023). Curcumin-loaded hydroxyapatite nanocomposite as a novel biocompatible shield for male Wistar rats from γ -irradiation hazard. *Chemico-biological interactions*, 370, 110328.
30. Al-Sherbini, A. S. A., El-Ghannam, G., Yehya, H., & Nassef, O. A. (2019). Optical and magnetic studies of $\text{Fe}_3\text{O}_4/\text{Au}$ Core/Shell nanocomposites. *International Journal of Nanoscience*, 18(05), 1850033.
31. Ji, D., Xiao, C., An, S., Zhao, J., Hao, J., & Chen, K. (2019). Preparation of high-flux PSF/GO loose nanofiltration hollow fiber membranes with dense-loose structure for treating textile wastewater. *Chemical Engineering Journal*, 363, 33-42.
32. Maalige, R. N., Aruchamy, K., Mahto, A., Sharma, V., Deepika, D., Mondal, D., & Nataraj, S. K. (2019). Low operating pressure nanofiltration membrane with functionalized natural nanoclay as antifouling and flux promoting agent. *Chemical Engineering Journal*, 358, 821-830.
33. Tischer, A. M., Ferreira, R. R., Ribeiro, J. G., dos Santos Rosa, D., & Paulino, A. T. (2024). Green synthesis of an advanced composite membrane for the purification of water contaminated with potentially toxic metals. *Journal of Water Process Engineering*, 61, 105239.
34. Dadari, S., Rahimi, M., & Zinadini, S. (2022). Novel antibacterial and antifouling PES nanofiltration membrane incorporated with green synthesized nickel-bentonite nanoparticles for heavy metal ions removal. *Chemical Engineering Journal*, 431, 134116.